PNAS RESEARCH ARTICLE | AGRICULTURAL SCIENCES OPEN ACCESS

# Overlooked branch turnover creates a widespread bias in forest carbon accounting

Hyungwoo Lim[a,b,c,1], David Medvigy[d], Annikki Mäkelä[e], Dohyoung Kim[f], Timothy J. Albaugh[g], Aubrey Knier[h], Róbert Blaško[a,i], Otávio C. Campoe[j,k], Rashila Deshar[l], Oskar Franklin[a,b], Nils Henriksson[a], Kim Littke[m], Reimo Lutter[n], Christopher A. Maier[o], Sari Palmroth[e,h], Katrin Rosenvald[c], Robert A. Slesak[p], Arvo Tullus[c], and Ram Oren[e,h,q,1]

Affiliations are included on p. 8.

Edited by Donald Ort, University of Illinois at Urbana Champaign, Urbana, IL; received January 30, 2024; accepted September 9, 2024

**Most measurements and models of forest carbon cycling neglect the carbon flux associated with the turnover of branch biomass, a physiological process quantified for other organs (fine roots, leaves, and stems). Synthesizing data from boreal, temperate, and tropical forests (184,815 trees), we found that including branch turnover increased empirical estimates of aboveground wood production by 16% (equivalent to 1.9 Pg $Cy^{-1}$ globally), of similar magnitude to the observed global forest carbon sinks. In addition, reallocating carbon to branch turnover in model simulations reduced stem wood biomass, a long-lasting carbon storage, by 7 to 17%. This prevailing neglect of branch turnover suggests widespread biases in carbon flux estimates across global datasets and model simulations. Branch litterfall, sometimes used as a proxy for branch turnover, ignores carbon lost from attached dead branches, underestimating branch C turnover by 38% in a pine forest. Modifications to field measurement protocols and existing models are needed to allow a more realistic partitioning of wood production and forest carbon storage.**

net primary production | carbon sink | branch mortality | forest model | allometric

## Significance

Net primary production of forests, a major land carbon flux, is estimated in the field as the sum of biomass increment, i.e., net growth of live biomass over time, and biomass turnover, i.e., the production of biomass replacing loss through mortality. Despite its importance in forest carbon dynamics, both measurements and models have largely overlooked turnover of branch biomass in live trees. Synthesizing field-based data across global biomes and incorporating branch turnover in state-of-the-art models, our study demonstrates that the prevailing neglect of branch turnover leads to widespread biases in carbon flux estimates across global datasets and model simulations. Modifications to field measurement protocols and model simulations are needed to eliminate the systematic biases in projection of land carbon dynamics.

Forests are major land carbon sink (1) and account for more than half of the terrestrial net primary production (NPP) (2). Accurate assessment of forest carbon dynamics is critical to understanding the global carbon cycle (3). In forest ecosystem, the extent to which the carbon (C) trees incorporate into biomass contributes to the forest C sink depends on its persistence in trees and soil. Portions of total NPP associated with different tree organs range in persistence from short-term (flowers, most leaves, and fine roots), to mid-term (branches and cones), and long-term (stems and coarse roots). Models that do not accurately allocate C among organs of differing persistence generate biased estimates of C sequestration rates and storage (4–6). For example, misallocating C of mid-term persistence branch NPP to short-term persistence foliage may result in overestimating canopy leaf area and thus photosynthesis and NPP, while misallocating it to stems may result in overestimating long-term C storage. This example was chosen to reflect the now-prevalent approach of ignoring C used in replacement of branch mortality (i.e., turnover) in modeling C sequestration and storage (6).

Net primary production in forests is commonly estimated as the sum of biomass turnover and increment. Turnover refers to the portion of biomass mortality, the C flux from live to dead pools, which is replaced annually (7, 8), estimated based on litterfall collection (leaves, reproductive organs) and repeated soil coring (fine roots); increment refers to the net change in standing biomass over time, typically based on allometric functions driven by easily obtainable tree dimensions. Turnover of short-lived components can amount to a large portion of NPP, as is obvious where the pool size of an organ reaches a quasi-steady state yet some or all the pool is replaced annually. For example, based on published information (*SI Appendix*, Table S1) we estimated that foliage and fine roots accounted for 29% (5) and 25% (9), respectively, of global forest NPP (2), likely representing mostly turnover (10). Not surprisingly, these fast-turnover C pools have been uniformly accounted for in measurements and ecosystem models of NPP (8–11). In contrast, branch turnover has been mostly ignored despite some studies suggesting a substantial turnover rate, ranging among species from about 15 to 45% of aboveground wood NPP (12).

A literature search (Web of Science, based on "Net primary production" OR "NPP" AND "Forest" published from Jan. 2003 throughout Feb. 2023) produced 492 original articles relevant to forest NPP (*SI Appendix*, Table S2). Although some studies estimated branch litterfall, only four of 278 publications from field studies accounted for branch turnover—99% neglected branch turnover in NPP estimates. Among the 121 models (including several generations of some) used in 236 articles, four empirical and four process-based models

The authors declare no competing interest.

This article is a PNAS Direct Submission.



[1]To whom correspondence may be addressed. Email: hyungwoo.lim@slu.se or ramoren@duke.edu.

This article contains supporting information online at https://www.pnas.org/lookup/suppl/doi:10.1073/pnas.2401035121/-/DCSupplemental.

Published October 10, 2024.

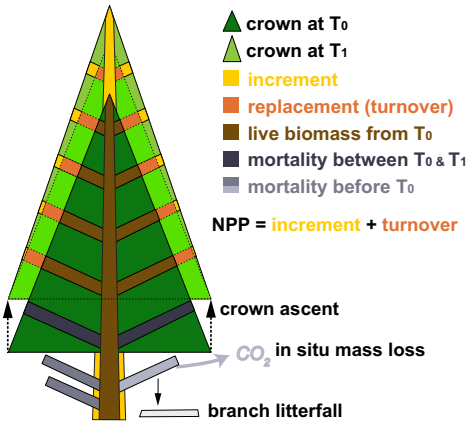


**Fig. 1.** Schematic description of the crown ascent model. New branches are produced where there is sufficient light, creating deeper shade mostly at the bottom of the crown. This causes mortality of low branches leading to crown ascent. Branches dying at the bottom are replaced with growth added to remaining branches, a replacement termed turnover. If the growth of the remaining and new branches exceeds branch mortality, the extra growth is termed increment. Dead branches often remain attached to stems for years to decades, undergoing in situ mass loss before falling. The crown ascent approach empirically estimates branch turnover (kg $y^{-1}$) based on the annual ascent rate of the crown base (m $y^{-1}$) with branch biomass per unit crown length (kg $m^{-1}$) at the lowest crown portion. This approach is a conservative estimate of branch turnover because shade-related turnover can also occur within crowns unrelated to the crown ascent.

accounted for branch turnover (29 publications in 20 y). Most of these models were not validated against measurements—at best results were compared against branch litterfall, which does not account for the lag between mortality and fall, lasting decades in some species, or for in situ mass loss of attached dead branches, a component of ecosystem respiration. Moreover, among the dynamic global vegetation models embedded in Earth System models used for estimating the fluxes in the global C budget, not one accounts for branch pools or branch turnover (3, 11). If the contribution of branch turnover to wood NPP is large enough to alter C allocation, this literature analysis suggests that biased NPP estimates are pervasive throughout global datasets and model simulations.

We hypothesize that neglecting branch turnover can lead to underestimated NPP from measurements and overestimated long-term stem C storage in model predictions. The objectives of this study were to i) estimate branch turnover across various forest types and spatial conditions, and ii) quantify the impacts of branch turnover on estimates of aboveground wood NPP. Furthermore, iii) we employed two process-based models to simulate stem wood biomass accumulation with or without including branch turnover.

We compiled unique datasets on repeated tree measurements (183,738 trees) that include the height of the crown base (14,627 trees) and on-site tree harvesting (1,077 trees) from 278 forest plots (dominated by eight species) in 21 long-term experiments. All experimental sites were even-aged forests, where a single species dominates the stand. We estimated annual branch turnover according to a crown ascent approach (13–15), whereby most branch turnover occurs at the crown base as it ascends while older, larger branches at the bottom gradually die (Fig. 1). The crown ascent approach is based on the branch autonomy theory (16), whereby branches cannot become a sink for carbohydrates produced elsewhere in the crown, and branches die as their solar energy capture is insufficient for a positive net C balance. The outcome is readily observable in even-aged single-species stands. This approach empirically quantifies branch turnover (kg $y^{-1}$) based on a combination of the annual ascent rate of the crown base (m $y^{-1}$) and branch biomass density in the lowest crown portion (biomass per unit length; kg $m^{-1}$). Because shade-related turnover can also occur within crowns unrelated to the crown ascent, the crown ascent approach provides a conservative estimate of branch turnover, relevant from the time crown ascent begins (commonly after canopy closure) until height growth and crown ascent slows to a stop. We thus estimated how much the crown ascent approach underestimates true branch turnover via mortality above the ascending base, using a unique dataset of 12 y of direct measurements of annual branch turnover based on >3,000 branches along the entire crowns of 80 shade-intolerant *Pinus taeda* trees (17). In addition, based on widely used process-based models, a "big-leaf" model, PREBAS (18), and a vegetation demographic model, Ecosystem Demography 2 (ED2) (19), we assessed how much stem biomass would be overestimated if C from branch turnover was misallocated to C accumulation in stems, the longest persistence tree-based C storage in forests.

## Results

**Branch Turnover of Trees and Stands.** We assessed field datasets in three ways: i) estimating annual branch turnover of monitored individual trees, ii) scaling the turnover to stands, and iii) quantifying contribution of branch turnover to branch NPP and total aboveground wood NPP.

The distributions of the branch biomass density, crown ascent rates, branch turnover, and the annual turnover rate of branch biomass (annual turnover per unit branch biomass, $\lambda_B$; $y^{-1}$) of individual trees were right-skewed and best fitted with a gamma distribution (Fig. 2 *A*–*C*) (15). $\lambda_B$ varied among species, ranging from 0.7% $y^{-1}$ in suppressed, shade-tolerant boreal *Picea abies*, taking 143 y to replace all branches, to 176% $y^{-1}$ of a shade-intolerant *Eucalyptus grandis* in a tropical plantation, doing so in ~7 mo (Fig. 2*A*). The variation of $\lambda_B$ among species was driven primarily by that of annual crown ascent rate (Fig. 2*B*), which varied more than branch biomass density (Fig. 2*C*).

Summing all individuals at each site, branch turnover was upscaled to the stand (i.e., to ground area; Fig. 2 *D*–*F*). Across the plots of all experiments, stand-scale $\lambda_B$ was 14 ± 19% $y^{-1}$ (mean ± 1 SD, n = 278), ranging from 0.5% $y^{-1}$ in the *P. abies* forest to 86% $y^{-1}$ in the *Eucalyptus* plantation, the latter replacing the entire branch biomass in 14 mo (Fig. 2*D*). Applying site-specific allometric equations to repeated field survey data, we found that branch turnover accounted for 51 ± 26% of branch NPP (Fig. 2*E*) and 13 ± 9% of aboveground wood NPP (Fig. 2*F*).

**Empirical Model of Annual Branch Turnover.** We accounted for variation across sites using variables widely employed for describing growth dynamics in forests (height increment and stand density) in both empirical and modeling studies. Partitioning the data into two broad categories of shade tolerance resulted in clearly different estimates of $\lambda_B$ and patterns explainable by height increment and stand density (Fig. 3). In stands of shade-intolerant species, $\lambda_B$ was related to height increment following a 4-parameter logistic curve (Fig. 3*A*); the unexplained residuals were related to size-normalized stand density (Fig. 3*B*) (20). In stands of shade-tolerant species, a linear model was better than a logistic model (Fig. 3*C*) and the residuals were associated with actual stand density (Fig. 3*D*). Overall, these four independent variables (height increment, two stand density expressions, and species type) explained 96% of the total variation in $\lambda_B$ across species, stand and site conditions (including different treatments), and biomes, showing no pattern in the residuals of predicted vs. measured values (*SI Appendix*, Fig. S1).

Spatially, the ratio of branch turnover to branch NPP and to aboveground wood NPP decreased with increasing crown length-to-tree height ratio (*SI Appendix*, Fig. S2), with similar

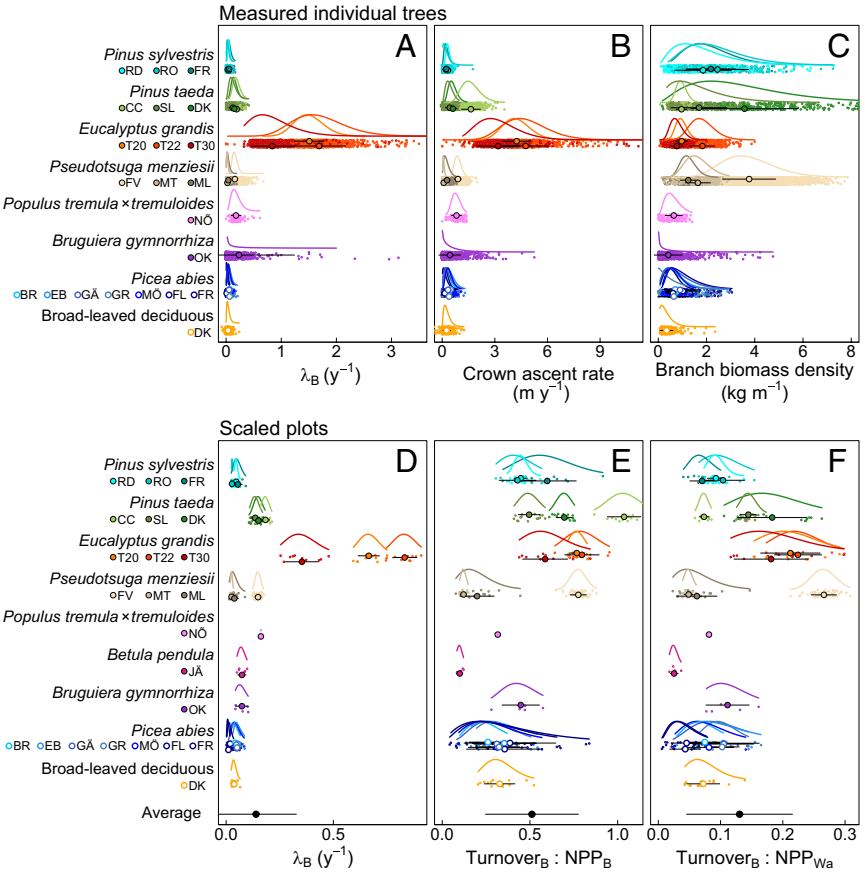


**Fig. 2.** Variable distributions at consecutively measured individual trees (*A*–*C*) and scaled plots (*D*–*F*). Distributions at measured individual trees of (*A*) annual turnover rate of branch biomass ($\lambda_B$), (*B*) annual ascent rate of crown base, and (*C*) branch biomass density per unit length of the live crown section at the bottom of the live crown. Distributions at scaled plots of (*D*) $\lambda_B$, (*E*) branch turnover ($Turnover_B$) relative to net primary production (NPP) of branches ($NPP_B$), and (*F*) that of aboveground wood NPP ($NPP_{Wa}$). Variables follow gamma distributions (solid lines), of which shape and scale were estimated based on mean (circles) and variance of the variables. Symbols with error bars represent averaged values for each site and ±1 SD, respectively, based on spatial variation among measured individual trees averaged across the monitoring periods (*A*–*C*) and among plots within a site (*D*–*F*). Detailed information on the abbreviation of each site and value estimates is given in *SI Appendix*, Tables S3 and S5.

slopes in both shade-tolerant and -intolerant species ($P = 0.374$ relative to branch NPP; $P = 0.057$ relative to the wood NPP).

**Evaluating the Crown Ascent Approach and Estimating In Situ Mass Loss of Dead Branches.** Using 12-year-long direct measurements of annual branch turnover along entire crowns of *P. taeda* trees, we found that the crown ascent approach captures 84 ± 2% of *true* branch turnover, occurring in the bottom 20% of the crown, regardless of crown shape or size (both varying among irrigation × fertilization treatments; line forced through zero, intercept $P = 0.093$; n = 781; Fig. 4 and *SI Appendix*, Fig. S3). We also estimated the amount of C lost from dead branches while attached to trees at another *P. taeda* forest, the Duke Free-Air $CO_2$ Enrichment (FACE) site, as the difference between the estimated branch turnover and the sum of branch litterfall and changes of attached dead branch pool (Fig. 5). We calculated two estimates, one based on the crown ascent model only and one including an estimate of within-crown branch turnover (+19%), not captured by the crown ascent. The in situ mass loss during the period between branch death and fall was estimated as 27 ± 16% (mean ±1 SE; n = 4) of the branch turnover, or 38 ± 13% when within-crown turnover is included (*Materials and Methods*).

**The Effect of Branch Turnover on Modeled Stand C Sink.** Not accounting for branch turnover in the 100-y-simulation of biomass accumulation, thus directing the ignored branch biomass turnover to stem biomass production, PREBAS and ED2 overestimated stem biomass of the shade-tolerant species by 19% and 9%, respectively (Fig. 6 *A* and *B*). Ignoring the branch turnover caused a greater stem biomass overestimation of shade-intolerant than shade-tolerant species, amounting to 23% and 21%, respectively (Fig. 6 *C* and *D*). Although PREBAS and ED2 were parameterized and developed completely independently and had different model structures, their estimates of *P. abies* stem biomass accumulation when branch turnover is included were within 16% of each other over 100-y-simulation period, averaging within ~2% deviation from empirical yield table (21). Branch turnover affected aspects of stand structure other than biomass. In ED2, adding branch turnover caused stand density (the number of trees per unit ground area) to be 5% larger in the *P. taeda* stand and 10% larger in the *P. abies* stand after 100 y.

## Discussion

Branch turnover has been largely ignored in experiments and monitoring studies of forest ecosystems, and most models of tree growth, stand dynamics, and ecosystem C cycling (*SI Appendix*, Table S2). Based on our extensive datasets, we demonstrated that 14 ± 19% of the branch biomass is turning over annually with the ascent of the crown base (reaching 90% in a fast-growing *Eucalyptus* plantation; Fig. 2), consistent with findings from the few published studies (12). This crown ascent associated branch turnover amounted to 13 ± 9% of aboveground wood NPP (reaching ~30% in *Pseudotsuga menziesii* plantations; Fig. 2*F*). Such high

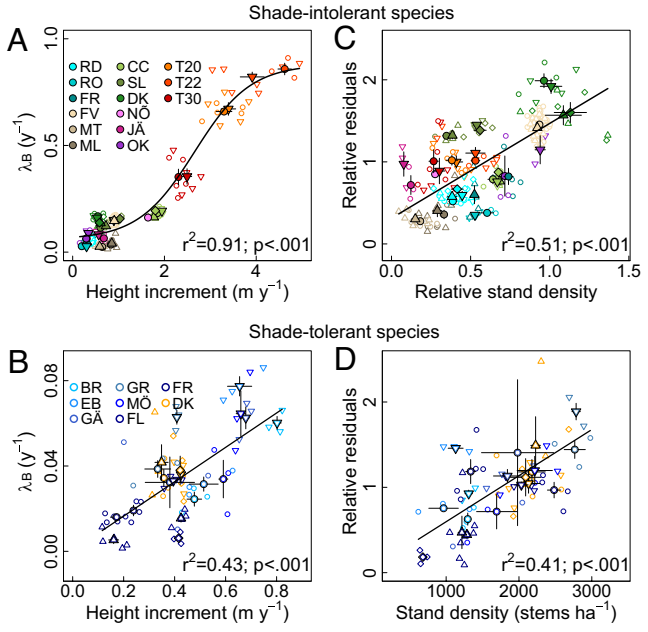


**Fig. 3.** Relationships for stand-scaled variables between (*A* and *B*) annual turnover rate of branch biomass ($\lambda_B$) and annual height increment and between (*C* and *D*) relative residuals (observed/predicted) and relative stand density to the theorical maximum density (shade-intolerant; *C*) and actual stand density (shade-tolerant species; *D*). Symbols with error bars represent averaged values for each treatment and ±1 SD, respectively, based on spatial variation among replicated plots. Parameters were estimated based on replicate plots and are presented in *SI Appendix*, Table S4. Different symbols indicate treatments (see details in *SI Appendix*, Fig. S2).

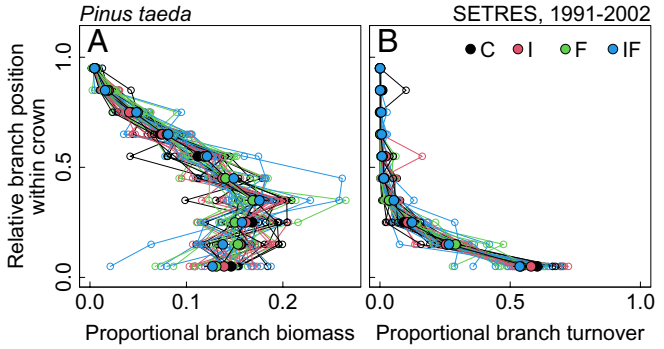


**Fig. 4.** Vertical distribution of (*A*) live-branch biomass and (*B*) turnover of individual trees from the SL site. In the SL site, branch turnover was directly measured annually for 12 y. (*A*) Vertical distribution of live-branch biomass as a proportion of the total branch biomass and (*B*) branch turnover in each crown layer as the proportion of total crown branch turnover. Vertical branch position was normalized to the crown length (0, *Bottom*; 1, *Top* of the crown). C, control; I, irrigation; F, fertilization; IF, irrigation and fertilization.

quantities demand attention. Although one forest growth model included branch turnover as early as 1997 showing that accounting for branch turnover improved predictions of height increment and biomass production (14), most models have ignored branch turnover.

We demonstrated using two differently structured forest growth models that ignoring the branch turnover may result in overestimation of stem production (Fig. 6). Absent branch turnover, calibrating either model by forcing a match with observed stem biomass accumulation, the C unallocated to branch turnover would have been allocated to other processes. In such case, ignoring branch turnover in model simulations would potentially result in overestimation of respiration, C allocation to mycorrhizal and other rhizosphere organism (22), or turnover of other organs. Otherwise, it would require model adjustments causing underestimation of canopy photosynthesis. The two models used here had different treatments of allocation and branch turnover. PREBAS included crown ascent and subsequent branch turnover. Given the model structure in PREBAS, we deliberately reallocated to stems the NPP saved by ignoring branch turnover, making the increase in stem growth an upper limit. Consistent with earlier PREBAS results (14), height growth rates and maximum height become more similar to observations when branch turnover is included. The other model we used, ED2, does not include branch turnover in its default version. In this way, it is similar to many other current models (*SI Appendix*, Table S2). When we implemented branch turnover in this study, allocation to branches was prioritized at the same level as allocation to stem but had a lower priority than allocation to leaves and fine roots (*Materials and Methods*). The simulated branch turnover in ED2 was an emergent process based on individual-tree height increments and allometric relations. ED2 simulations showed that accounting for branch turnover reduces modeled C storage in the long-lasting stem biomass pool, in turn affecting self-thinning and stand dynamics.

Regardless of the model's philosophy and structure, ignoring branch turnover is to the detriment of model performance and how closely model results match or estimate C pools and fluxes.

Our empirical estimates based on the crown ascent approach assume that the mortality occurring at the bottom of crowns is replaced throughout the crown as the crown ascends (Fig. 1). This approach is correct for the *Eucalyptus* plantations, where most of the branches were replaced annually. In other sites, however, twigs and branches may die throughout the crown; moreover, when trees reach maximum height, most of the turnover may occur within the crown rather than at the bottom of the crown (16). We quantified the underestimation inherent to the crown ascent approach using a unique dataset on *P. taeda* where irrigation and fertilization treatments caused a wide range of stand characteristics (17). The stand was young, and the time series began at a low relative stand density, and thus, the crown ascent rate was lower for this shade-intolerant species than under typical, higher-density conditions. As a result, turnover in the crown unrelated to the crown ascent contributed a relatively high proportion (16%) of the branch turnover, a quantity that was similar in all treatments (Fig. 4 and *SI Appendix*, Fig. S3). Until similar studies are performed, this may be used for similar species as the upper limit of branch turnover unaccounted for by the crown ascent. We note that the estimate we offer does not include the mortality from

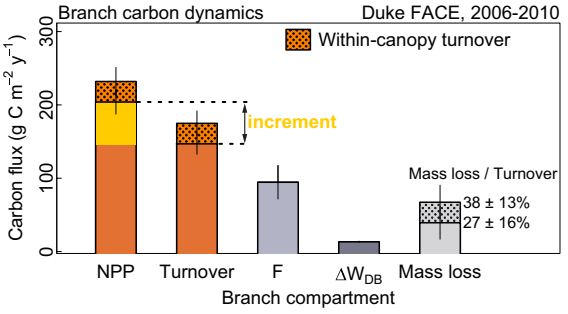


**Fig. 5.** Branch carbon dynamics in the Duke FACE site. Net primary production (NPP) of branch biomass, turnover of branch biomass, branch litterfall (F), annual changes of attached dead branch biomass pool ($\Delta W_{DB}$), and in situ mass loss of dead branches, the latter estimated as turnover − (F + $\Delta W_{DB}$). Branch NPP is the sum of branch biomass increment estimated based on allometric functions and turnover. The F and $\Delta W_{DB}$ were stable over the monitoring years (2006–2010; *SI Appendix*, Fig. S4). Based on the SL site data, within-canopy branch turnover was estimated as 19% of the crown ascent-induced branch turnover (dotted orange bar; for detailed analysis, see Fig. 4 and *SI Appendix*, Fig. S3).

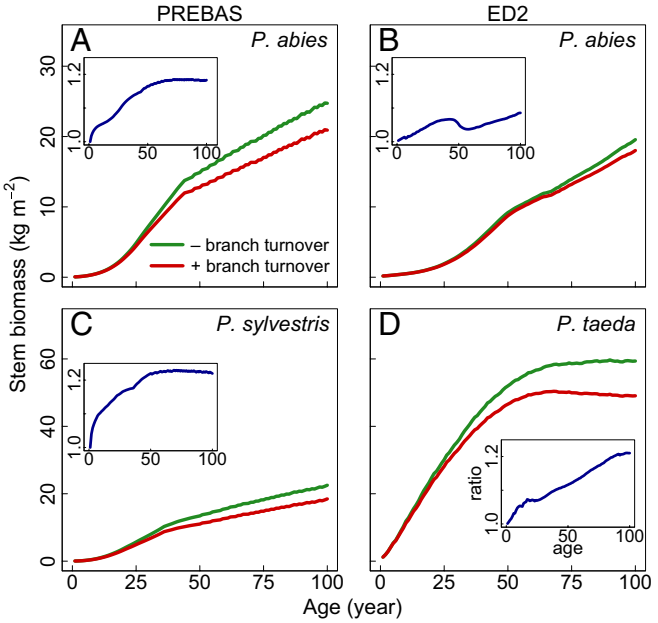


**Fig. 6.** Model simulations of stem biomass over 100 y. (*A* and *B*) Simulations of shade-tolerant species, a boreal *Picea abies* stand in southern Finland using PREBAS (*A*) and ED2 (*B*). (*C* and *D*) Simulation of shade-intolerant species, a boreal *Pinus sylvestris* using PREBAS (*C*) and a temperate *Pinus taeda* using ED2 (*D*). Inset figures present the ratio of the stem biomass between simulations without the turnover of branch biomass and those including the turnover.

diseases, insects, and severe weather events, and is not applicable to trees reaching maximum height and stable crown base.

Why has the turnover of branch biomass been given so little attention, or treated so casually in modeling? The likely culprit is the scarcity of reliable data demonstrating the significance of this flux (12, 23). The reason for this, in turn, is that branch turnover is difficult and time consuming to measure well. Indeed, the quantity typically measured in forests is branch litterfall (24), not branch turnover. However, during the period between death and fall, branches are losing mass to insects and microbial decomposers at a rate which varies dependent on branch properties and the environment. Not surprisingly, branch litterfall greatly underestimates branch turnover; in one temperate forest, branch litterfall accounted for only 14% of branch turnover (25). Thus, branch litterfall, sometimes used as a proxy for branch turnover, may cause a significant bias in estimates of component C fluxes.

Nevertheless, measurements of branch litterfall can be useful under certain conditions for estimating mass loss in situ. This estimate can be added to component-based estimates of ecosystem respiration and compared to eddy covariance measurements for assessment of the C budget closure. For example, under conditions in which the accumulation rate of attached dead branch biomass is known, the amount of mass loss of these branches can be estimated as the difference between branch turnover and a sum of branch litterfall and the increment of the attached dead branch pool. Based on the detailed Duke FACE *P. taeda* data over the five-year period during which canopy leaf area (26), buildup of dead branch biomass, and litterfall were stable (*SI Appendix*, Fig. S4), we found that 67 g C m$^{-2}$ was lost annually before branches fell when including the within-crown turnover for this species (Fig. 5). This represents in situ mass loss equivalent to 122% of fine root turnover (27) and 4% of eddy covariance-based estimate of ecosystem respiration at the site (28).

The rate of annual branch turnover per unit branch biomass ($\lambda_B$) is useful for constraining other portions of the C cycle in forest ecosystems. For example, Muukkonen & Lehtonen (29) devised a $\lambda_B$ model based on stand age for shade-intolerant *P. sylvestris* (averaging 2.7% y$^{-1}$) or a fixed rate of 1.3% y$^{-1}$ for shade-tolerant *P. abies*. Our empirical $\lambda_B$ model is based on variables reflecting the physiological response to increasing shading from the crown above (height increment; Fig. 3 *A* and *C*) and neighboring trees (stand density; Fig. 3 *B* and *D*). The variables explaining 96% of the spatial variation in $\lambda_B$ are commonly available from field measurements (30) and are used in most models (3, 11), thus simplifying their incorporation in current projects and models. We note that data for estimating interannual variation in both height growth and branch turnover are rare. Based on the most detailed study on branch demography of *P. taeda* (17), interannual variations in both quantities were small, and the coefficient of variation, CV, of $\lambda_B$ (6%) was much smaller than the spatial variation observed among stands of the same or different species (Figs. 2 and 3). Indeed, the variation in $\lambda_B$ is primarily driven by variation among sites, which are much larger than those observed within sites even including water and nutrient manipulations (CV of site-specific $\lambda_B$ averaging 10%, ranging 2 to 37% among all sites vs. 64% among species × sites). Thus, both temporal and within-site spatial variations are small relative to those among species × sites. Although this work is aimed primarily at coarse-scale modelers, we encourage experimentalists to add the necessary measurements so more robust datasets are created, allowing a better definition of temporal and local variation.

The relationships we offer are mostly based on data from even-aged forests composed of one or two species, precluding a thorough evaluation of the crown ascent model in multi-species, multi-aged stands of complex structure, or angiosperm species that have branching stems with diverse branch architectures. Two stands (FR and DK) represent the more typical conditions of mixed-species and ages, and only one stand represents angiosperm species with branching stems (OK). For FR and DK stands, we computed the stand density of subcanopy species based on the number of all trees in a plot because incoming light to the subcanopy is affected by the density of canopy trees (31), while the density of canopy species was computed based on their number only. This approach to accounting for density effects on branch turnover in different canopy layers of mixed-species stands seems promising and the crown rise approach seems applicable regardless of branching architectures because there was no indication of bias in the residuals of these stands when employing the general model (*SI Appendix*, Fig. S1). The model may have worked in OK site because angiosperms growing in closed canopy stands, even those with multiple stems, grow principally upward and together, resulting in branches being replaced in a similar way as for single-stem trees. Nevertheless, including measurements of crown ascent and branch biomass density of the lower crown in forest productivity studies is a necessary step in reducing the uncertainty of NPP estimates and validating generality of the crown rise approach across plant functional types.

Our analysis shows that branch turnover plays a substantial role in C cycling across forest types, a large yet likely underestimated amount due to within-crown turnover unrelated to the crown ascent (Fig. 3). Considering our sites and species representative of global forests, we extrapolated the findings globally based on the average fraction of branch turnover to aboveground wood NPP (16 ± 12%) and forest-type area-weighted mean global ratio of aboveground wood NPP to total NPP (37 ± 3%; *SI Appendix*, Table S1). This estimate suggests that global branch turnover may amount to 1.9 ± 0.8 Pg y$^{-1}$, or 6 ± 2% of the global forest NPP (32.2 Pg y$^{-1}$) (2), equivalent to a 79 ± 31% of the global forest C sink (2.4 Pg y$^{-1}$) (1). A more conservative, lower-bound estimate of 0.36 ± 0.14 Pg y$^{-1}$ (1.1 ± 0.4% of NPP; equivalent to 15 ± 6% of the global sink)

is obtained when assuming no crown ascent and accounting only for within-crown turnover (~3% of aboveground wood NPP). The current imbalance in the global C budget (−0.6 Pg $y^{-1}$) (3) is caused by either underestimated sources or overestimated sinks. In the latter case, the uncertainty is largely attributed to uncertainty in the land sink strength (3). Considering these quantities, reallocating C from longer-term storage in stems to faster turning-over branches may help reduce this imbalance and motivates the incorporation of branch turnover into the C cycle assessments.

We recommend revising the sampling protocol of projects focused on biomass production, and C cycling and storage in forest ecosystems. At a minimum, tasks should be amended to include measurements to estimate the ascent rate of crowns and the branch biomass density per unit crown length at the lower crown. Additional sampling would allow estimating the C pool of attached dead branches and branch litterfall over time and, in turn, $CO_2$ loss to the atmosphere from in situ branch consumption by insects and decay. Also needed are modifications to existing models, allowing a more realistic partitioning of production between stems and branches. Given the observed dependence of branch turnover on height increment and stand density, such modifications should be especially tractable in size-structured forest and vegetation models (11).

## Materials and Methods

**Data Sources and Estimation of Biomass and Net Primary Production.** Consecutive measurements of dimensions of individual trees and derived site-specific allometric functions are essential for the analyses. We obtained datasets that (i) were accompanied by on-site tree harvests to derive site-specific allometric functions and branch biomass distribution along crowns and ii) included annual or periodic measurements of stem diameter, tree height (H), and height to the base of live crown made on each tree within a defined ground area. Together, these allow estimation of the ascent rate of the crown base, branch biomass turnover, and annual increment of branch and stem biomass.

The datasets matching the above requirements represent 183,738 individual trees and 1,077 on-site harvested sample trees from 278 treatment plots across 21 forests in four tropical, six temperate, and 11 boreal climates of commercially important species, in addition to a tropical mangrove forest (*SI Appendix*, Table S3): *Pinus sylvestris* [three sites, RD (32), RO (33, 34), and FR (35–37)], *P. taeda* [three sites, CC (38), SL (17), and DK (26)], *E. grandis* [three sites, T20, T22, and T30 (39)], *Pseudotsuga menziesii* [three sites, FV (40), MT, and ML (41)], *Populus tremula* × *tremuloides* [NÕ (42)], *Betula pendula* [JÄ (43)], *Bruguiera gymnorrhiza* [OK (44)], and *Picea abies* [seven sites, BR, EB, GÄ, GR, MÖ (45, 46), FL (47, 48), and FR (35–37)]. Datasets cover stand age between 4.6 to 100 y and observation periods lasting 1.6 to 14 y.

Using the harvested, sample trees, we developed site × treatment-specific allometric functions for branch and stem biomass using stem diameter at 1.3 m (D) and H or length of live-crown (LC) as independent variables (*SI Appendix*, Tables S6 and S7 and Fig. S5). Crown of each harvested tree was vertically divided into 3 to 7 equal length strata (one stratum for *E. grandis*), and a relative proportion of branch biomass at each stratum to total branch biomass was estimated. Applying the allometric functions to the repeated measurements of each standing tree's dimensions, we estimated their branch and stem biomass. Annual net biomass increment was estimated as the difference in biomass between two measurement years divided by the number of years in the interval. Branch biomass density of the lowest crown section (branch biomass per unit length in kg $m^{-1}$) was estimated based on a combination of branch biomass estimates of the tree, the proportion of branch biomass of the lowest crown section, and the length of the stratum. Following a crown ascent approach (13–15), branch turnover was estimated based on branch biomass density of the lowest crown section, multiplied by the annual ascent rate of the crown base (m $y^{-1}$). The annual turnover rate of branch biomass ($\lambda_B$) was defined as annual branch turnover per unit standing branch biomass at the start of the year. Net primary production (NPP) of stem or of branches was estimated as biomass increment plus turnover (kg $tree^{-1}$ $y^{-1}$).

Scaling to ground area (stand) at six sites (T20, T22, T30, SL, DK, and NÕ) where H and LC were measured on all trees, we summed quantities estimated for the individuals and divided the sum by the plot area. In the boreal sites (RD, RO, FR, BR, EB, GÄ, GR, MÖ, and FL) and northwestern pacific MT, ML sites, H and LC were measured on a subset of trees (between 6 and 35 per plot × year, or ~20% of total number of trees; *SI Appendix*, Table S8), while D was measured on all the trees. Using the measured dimensions of the subsets, we developed a H-D relationship for each plot × treatment × year combination, following Näslund's relationship for boreal sites (49) and a power function for the MT and ML sites (*SI Appendix*, Fig. S6). LC was estimated using a relationship between live-crown ratio (LCR; LC $H^{-1}$) and D obtained in each sampling subset, unless the slope of the relationship was not different from 0, in which case mean LCR was used. Applying the H-D relationships and LCR, we estimated both H and LC of all trees in these sites. For the CC and FV sites, D and H were measured on all trees, but height to the base of live crown only on a subset of trees. We therefore used the same approach as in the boreal sites to estimate LC for the remaining trees. For JÄ site, measurements were made on D, H, and LC in 2019 but only D and H were measured in 2017. In addition, 12 and 14 trees were destructively harvested in 2019 and 2017, respectively. To predict LC, we developed a H-LC relationship for each year using the harvested sample trees. The model was validated against the measured LC in 2019 ($r^2 = 0.972$, $P < 0.001$; *SI Appendix*, Fig. S7). We then predicted LC of all trees for each year based on a combination of the relationships and the measured H. In the analysis, we used predicted LC for both years. Measured D and H, and estimated LC were used to estimate stem and branch biomass and annual net increment between sequential measurements, and turnover, which were summed and divided by the ground area to scale up to a stand level (kg $m^{-2}$ and kg $m^{-2}$ $y^{-1}$, respectively).

**Evaluation and Sensitivity Analysis of the Crown Ascent Model.** To evaluate the accuracy of the crown ascent model, we analyzed the dataset on *P. taeda* from the SL site with four fertilization × irrigation treatment combinations (17). In the experiment, demography of >3,000 branches had been monitored annually for 12 y, tracing individual branch and twig and quantifying turnover, on five trees in each of 16 plots (900 $m^2$ each), recording the vertical position, year of death, and biomass. We estimated gross production (live and dead biomass) and net production (live biomass) of branches with an increasing number of vertical crown layers, and the total annual branch turnover for each tree (*SI Appendix*, Fig. S3). Using these estimates, we first quantified potential errors of the crown ascent model by estimating vertical distributions of branch biomass and its turnover, within the crown.

When trees are harvested to characterize crown structure, the crown is typically divided vertically into several equal strata (33). The number of strata into which the crown is partitioned affects the mean branch biomass density at the lowest crown section, thus affecting the estimated turnover using the crown ascent approach. We performed a sensitivity analysis of branch biomass density (biomass per unit crown length of the lowest layer), partitioning the crowns to an increasing number of crown strata (*SI Appendix*, Fig. S3). Our analysis showed that model predictions based on gross-branch biomass density (in which dead and live branches are combined along the crown) were consistently in a good agreement with the observations regardless of the number of strata (*SI Appendix*, Fig. S3*A*), suggesting that using the gross density at the base of the crown coupled with a fixed crown ascent rate, overestimated branch turnover at the bottom by a similar amount to the mortality occurring throughout the crown. However, such detailed information is extremely rare. A more practical approach is to model branch turnover based on live-branch density at the crown base. This analysis showed our estimate to be linearly related to the observations yet reflected underestimation regardless of the number of crown layers. The changing biomass density with increasing number of layers coupled with the distribution of branch turnover along the crown resulted in increasing negative bias in estimation of branch turnover, ranging from the above-mentioned 84% of observed values using three layers to 74% (SE = 1.7%) using nine (inset *SI Appendix*, Fig. S3*B*).

**Analysis of the Spatial Variations of the Annual Turnover Rate of Branch Biomass ($\lambda_B$).** We evaluated the spatial variability potentially caused by species, site, and treatment, after finding smaller temporal variation relative to the spatial variation in the detailed data from SL site (coefficient of variance 6% vs. 13%, respectively). Moreover, in slow-growing forests such as those in our boreal sites,

interannual variation of crown ascent rates may be as small as the measurement uncertainty; we therefore calculated mean branch biomass and annual turnover over multi-year measurement periods. Cross-site variation of $\lambda_B$, separately for shade-intolerant and -tolerant species, were related sequentially to two independent variables, annual height increment as a proxy of site productivity, and stand density (the number of trees per unit ground area) as a proxy of competition and related mortality. For shade-intolerant species, we employed a 4-parameter logistic function and annual mean height increment as the best predictor variable. Because of the large variation of productivity among sites and species, the variance of the residuals increased with increasing predicted values and were thus normalized by the response variable. Model selection was determined based on residual distribution and the coefficient of determination. Variation of the normalized residuals were then regressed against relative stand density; an expression calculated as the current stand density divided by a theoretical maximum density of trees of the same mean size, the latter dependent on species. We used Reineke's model (20) to estimate the maximum stand density for each plot with a default coefficient of 1.605, excepting boreal (1.660) (50) and mangrove (1.618) (44) plots. For shade-tolerant species, linear regressions were used with annual mean height increment, and the normalized residuals were related to actual stand density. The final residuals were then analyzed using a generalized linear model to examine the effects of treatments on $\lambda_B$ for each site.

We related the ratio of branch turnover to branch NPP and to NPP of aboveground wood biomass to the live-crown ratio using a linear regression.

**Estimation of In Situ Mass Loss of Attached Dead Branches.** We obtained measurements of branch litterfall from the Duke FACE site (26, 51) in which atmospheric [$CO_2$] was elevated by 200 ppm in four plots (n = 4 each in elevated and ambient treatments), and half of each plot was supplied annually with ammonium-nitrate. Litterfall collection and processing was fully described in ref. 51. We concentrated on the final five-year period (2006–2010) during which canopy leaf area, branch turnover, annual buildup of dead, attached branches, and litterfall were stable (*SI Appendix*, Fig. S3), and the crown base is high (the height to crown base ranging from 14.0 to15.5 m over the five years). Dead branch pools that are attached to stems were predicted based on allometric equations for dead branches (*SI Appendix*, Fig. S8). We estimated mass lost in situ as

$$\left[Turnover - \left(F + \Delta W_{DW}\right)\right] \times 0.507,$$

where $F$ is branch litterfall, $\Delta W_{DW}$ is change of attached dead branches, and the constant is C concentration of dead branches at the site (50.7 ± 1.7% of dry mass). We then contrasted the mass loss in the ambient-unfertilized (i.e. the reference) plots with annual fine root turnover (130 g DW $m^{-2}$ $y^{-1}$) (27) of which C content amounted to 43.08 ± 1.52% and ecosystem respiration measured by the eddy covariance technique (1,656 g C $m^{-2}$ $y^{-1}$) (28).

**Branch Turnover in the Context of Global Forest Net Primary Production and Carbon Sink.** We contrasted branch turnover with estimates of global forest NPP of 32.2 Pg C $y^{-1}$ (2) and forest C sink of 2.4 Pg C $y^{-1}$ (1). Global forest fine root NPP (7.9 Pg C $y^{-1}$) (9), and foliage NPP (9.4 ± 0.5 Pg C $y^{-1}$) and aboveground wood biomass NPP (11.8 ± 0.4 Pg C $y^{-1}$) were estimated based on the mean annual NPP for each biome multiplied by the corresponding area (*SI Appendix*, Table S1) (5). Errors of the estimates were propagated based on a combination of the original source of NPP (5) and our error estimates of the mean ratio of branch turnover to aboveground wood NPP (Fig. 2*F*). Because of poor coverage of tropical species and stands, we extrapolated the findings globally based on the overall average fraction of branch turnover to aboveground wood NPP without including branch turnover (16 ± 12%) and forest-type area-weighted fraction of aboveground wood NPP to total NPP (37 ± 3%; *SI Appendix*, Table S1)–biome-specific weighted fraction of branch turnover to aboveground wood NPP was estimated as 21 ± 9%.

**Statistical Analyses.** All statistical analyses were performed using R (v. 4.2.2): The *nls* function was used to estimate the parameters of the 4-p logistic regression, *lm* for linear regression, and *lme* in the nlme package (v. 3.1-163) for split-plot ANOVA tests. Residual distributions were checked visually by plotting against predicted values and determined using *shapiro.test* and *gamma_test* functions in the goft package (v. 1.3.6). The *glm* and *anova* functions were used to determine the effect of treatments on the residuals. Estimated parameters of $\lambda_B$ model are presented in *SI Appendix*, Table S4, and mean estimates and SD of each treatment-site are presented in *SI Appendix*, Table S5.

**Model Simulations.** PREBAS combines a forest growth model (14, 52), and a forest gas flux model (53) to simulate forest growth based on its C balance. The tree growth model is cohort-based and can be applied to different stand structures (54) but is here used as a stand mean-tree model by species, applied to shade-intolerant *Pinus sylvestris* or shade-tolerant *Picea abies* forest. The model derives growth from C acquisition and allocation at an annual time resolution. Mean trees are described in terms of 13 variables, including biomass components and crown, stem, and root system dimensions. Growth is assumed to follow from net annual photosynthesis, allocated to the different biomass components to maintain structural rules. The gas flux model is an ecosystem model of intermediate complexity (53) at a daily time-step interlinking gross primary production, evapotranspiration, and soil water. The gas flux model has been calibrated using gross primary production and water balance data from 10 eddy covariance sites in Fennoscandia (55) and the whole PREBAS model has been calibrated using growth experiments in Finland (21).

Branch mortality is an integral part of the PREBAS model (52, 56). The model describes the tree as consisting of foliage, fine roots, and wood. Wood is divided into branches, coarse roots, and stems, and the stems are further divided into stem inside the crown and stem below the crown. Foliage mass is linked through the pipe model to cross-sectional area at crown base, and branch mass also depends on this cross-sectional area, as well as mean branch length. In addition, an allometric relationship is assumed between foliage mass and crown length. The processes of height growth and branch replacement are tightly related. When trees compete for light, growing taller and increasing leaf area at the crown top, bottom branches are shaded and die. As branches at the base of the crown die, trees replace their leaf area by growing taller, accommodating new branches and allometrically forcing increase in diameter. PREBAS uses remaining light at crown base as a measure of competition; with increasing competition and branch mortality at the base of the crown, PREBAS allocates C to branch production replacing these branches throughout the crown as well as extending the crown upward. The end result is an ascending crown accompanied by investment of C in height and diameter increment. Because branch turnover is an integral part of the model, it cannot be "turned off"–other than assuming no crown ascent, such as in an unshaded situation. In order to analyze the significance of ignoring branch turnover with PREBAS, we simulated stand growth using the standard model, calculated the annual branch turnover predicted by the model, and then added this to stem growth. The result indicates how much more stem growth would be predicted if branch turnover was not accounted for but instead, the C used for the turnover was used for stem growth.

The simulations were carried out for *Picea abies* and *Pinus sylvestris* stands in southern Finland, starting from a planted seedling stand and simulating for 100 y without management. In both cases, the sites were on a medium fertility, moist, herb-rich site classified as *Vaccinium myrtillus* site (57). These sites are characterized by podzol soils with high sand or moraine content. We used daily weather data (photon flux density, mean temperature, vapor pressure deficit, and precipitation) interpolated from weather stations and representing the period 1970–2000, which was repeated to cover the whole period. The data came from the Finnish Meteorological Institute.

The Ecosystem Demography 2 model (ED2) (19, 58) falls within a class of models called "Vegetation Demographic Models"(11), which means that it explicitly simulates demographic variation. Thus, the model resolves competition between plant functional types, variation in tree growth rates within a stand, and variation of tree growth rates across stands of different densities. ED2 has been used to simulate temperate forests of the United States (19, 59), boreal forests (60), and tropical forests (61–64). The model conceptualizes vegetation in terms of "cohorts." A cohort is a collection of plants of the same size and species located in the same resource environment. Cohorts compete for light, water, and nutrients and the model computes rates of resource acquisition. After acquiring resources, cohorts increase in size and reproduce. Size growth is characterized by increases in stem diameter, height, wood biomass, and maximum leaf biomass according to allometric relationships (58). Growth in ED2 takes place in two stages, and the first stage is cohort-level growth of leaves and fine roots. Leaves and fine roots grow simultaneously according to a prescribed leaf-to-fine root ratio. Each cohort has a maximum leaf (and fine root) biomass that is determined by its stem diameter.

The model prioritizes allocation to leaves and fine roots over allocation to wood until the leaf and fine root biomass pools reach their allometrically-defined targets. The second stage of growth, involving stem, branches, and reproduction, is only reached if cohorts are at their maximum leaf and fine root biomass for their size. Thus, if branch turnover is neglected, ED2 can only allocate the C that would have gone to branch turnover to stem production and reproduction.

As a demographic model, ED2 requires an initial condition that corresponds to the current vegetation state. The minimum initial condition consists of stem diameter and species assignment for all the trees in the stand. Additionally, meteorological data must be provided to drive the model over the time frame of the simulation. These data include temperature, precipitation, $CO_2$ concentration, relative humidity, pressure, wind speed, downward shortwave radiation, and downward longwave radiation. These meteorological drivers are typically provided at the 30- or 60-min time scale. The minimum required soil information includes sand and clay content and %C.

We selected two sites for ED2 simulations. The first site was the shade-tolerant *Picea abies* site, the same southern Finland simulated by PREBAS. The second site was Duke Forest, where we simulated the development of a *P. taeda* stand. The published versions of ED2 do not explicitly include branch biomass or branch turnover. For *P. taeda*, we estimated branch biomass according to Gonzalez-Benecke et al. (65) using stem diameter and age as independent variables. For *Picea abies*, we estimated branch biomass according to Repola (66) using stem diameter and tree height as independent variables. We then carried out simulations with and without branch turnover. Simulations without branch turnover corresponded to the current default version of the model, so no changes to the code were required. In simulations with branch turnover, we edited the code so that the annual branch turnover rate ($\lambda_B$) was prescribed using results from *SI Appendix*, Table S4 for both shade-intolerant and shade-tolerant species types. Allocation to leaves and fine roots took precedence over allocation to branches and stem, until leaves and fine roots reached their maximum pool size. We note that for these species, relative allocation to reproduction was small (<5%), so most of the C that would have gone to branch turnover goes to stem. We solved for branch and stem NPP simultaneously because of the explicit dependence of $\lambda_B$ on annual height increment. ED2 requires sub-daily meteorological data as input, so we could not use the daily data from the Finnish Meteorological Institute. Therefore, for the *Picea abies* simulations, we obtained half-hourly data from the ECMWF ERA-40 Reanalysis (Copernicus Climate Change Service 2022) (67). For the *P. taeda* simulations, we used data from an in situ weather station. For both sites and species, $\lambda_B$ was an emergent process and depended on rates of cohort-level height growth. All simulations were carried out for 100 y.

**Data, Materials, and Software Availability.** Computation code (R) and data used for stand scale analyses have been deposited in SafeDeposit (68).

**ACKNOWLEDGMENTS.** This study was partly supported by Kempestiftelserna (JCSMK23-0136). H.L. was financed by FORMAS (Grant number 2020-02319). Financial support for S.P. and R.O. was provided by the ACCC Flagship–University of Helsinki, funded by the Academy of Finland (Grant number 337549). The Duke Forest FACE project was supported by the Office of Science (BER) Terrestrial Ecosystem Sciences (TES) Program of the US Department of Energy (DOE), under contract number DE-AC05-00OR22725. R.L. was financed by Estonian Research Council Grant PSG730. K.R. and A.T. were supported by the Estonian Research Council (Grant number PRG1434).

Author affiliations: [a]Department of Forest Ecology and Management, Swedish University of Agricultural Sciences, Umeå SE-901 83, Sweden; [b]International Institute for Applied Systems Analysis, Laxenburg A-2361, Austria; [c]Department of Botany, University of Tartu, Tartu EE-50409, Estonia; [d]Department of Biological Sciences, University of Notre Dame, Notre Dame, IN 46556; [e]Department of Forest Sciences, University of Helsinki, Helsinki FI-00014, Finland; [f]Department of Geography, State University of New York at Buffalo, Buffalo, NY 14261; [g]Department of Forest Resources and Environmental Conservation, Virginia Polytechnic Institute and State University, Blacksburg, VA 24061; [h]Division of Environmental Sciences & Policy, Nicholas School of the Environment, Duke University, Durham, NC 27708; [i]Slovak Environment Agency, Banská Bystrica 975 90, Slovakia; [j]Department of Forest Sciences, Federal University of Lavras, Lavras, MG 37200, Brazil; [k]Department of Forestry and Environmental Resources, North Carolina State University, Raleigh, NC 27695; [l]Central Department of Environmental Science, Tribhuvan University, Kirtipur 44618, Kathmandu, Nepal; [m]Stand Management Cooperative, School of Environmental and Forest Sciences, University of Washington, Seattle, WA 98195; [n]Chair of Silviculture and Forest Ecology, Institute of Forestry and Engineering, Estonian University of Life Sciences, Tartu EE-51006, Estonia; [o]Southern Research Station, United States Forest Service, Research Triangle Park, NC 27709; [p]Pacific Northwest Research Station, United States Forest Service, Olympia, WA 98512; and [q]Department of Civil & Environmental Engineering, Pratt School of Engineering, Duke University, Durham, NC 27708

Author contributions: H.L. and R.O. designed research; H.L. and R.O. performed research; D.M., A.M., D.K., T.J.A., A.K., R.B., O.C.C., R.D., O.F., N.H., K.L., R.L., C.A.M., S.P., K.R., R.A.S., and A.T. contributed new reagents/analytic tools; H.L., D.K., T.J.A., and R.O. analyzed data; H.L., D.K., T.J.A., A.K., R.B., O.C.C., R.D., N.H., K.L., R.L., C.A.M., S.P., K.R., R.A.S., and A.T. collected and/or curated original datasets on field measurements and tree harvests; and H.L., D.M., A.M., and R.O. wrote the paper.

1. Y. Pan *et al.*, A large and persistent carbon sink in the world's forests. *Science* **333**, 988–993 (2011).
2. I. C. Prentice *et al.* "The carbon cycle and atmospheric carbon dioxide" in *Climate Change 2001: The Scientific Basis, Contribution of Working Group I to the Third Assessment Report of the Intergovernmental Panel on Climate Change*, J. T. Houghton *et al.*, Eds. (Cambridge Univ Press, NY, 2001).
3. P. Friedlingstein *et al.*, Global carbon budget 2022. *Earth. Syst. Sci. Data.* **14**, 4811–4900 (2022).
4. M. G. D. Kauwe *et al.*, Where does the carbon go? A model–data intercomparison of vegetation carbon allocation and turnover processes at two temperate forest free-air $CO_2$ enrichment sites. *New Phytol.* **203**, 883–899 (2014).
5. S. Luyssaert *et al.*, $CO_2$ balance of boreal, temperate, and tropical forests derived from a global database. *Glob. Chang. Biol.* **13**, 2509–2537 (2007).
6. F. Montané *et al.*, Evaluating the effect of alternative carbon allocation schemes in a land surface model (CLM4.5) on carbon fluxes, pools, and turnover in temperate forests. *Geosci. Model. Dev.* **10**, 3499–3517 (2017).
7. D. Binkley, M. Arthur, How to count dead trees. *Bull. Ecol. Soc. Ame.* **74**, 15–16 (1993).
8. D. A. Clark *et al.*, Measuring net primary production in forests: Concepts and field methods. *Ecol. Appl.* **11**, 356–370 (2001).
9. R. B. Jackson, H. A. Mooney, E.-D. Schulze, A global budget for fine root biomass, surface area, and nutrient contents. *Proc. Natl. Acad. Sci. U.S.A* **94**, 7362–7366 (1997).
10. T. A. M. Pugh *et al.*, Understanding the uncertainty in global forest carbon turnover. *Biogeosciences* **17**, 3961–3989 (2020).
11. R. A. Fisher *et al.*, Vegetation demographics in Earth System Models: A review of progress and priorities. *Glob. Change. Biol.* **24**, 35–54 (2018).
12. P. Y. Bernier, M. B. Lavigne, E. H. Hogg, J. A. Trofymow, Estimating branch production in trembling aspen, Douglas-fir, jack pine, black spruce, and balsam fir. *Can. J. For. Res.* **37**, 1024–1033 (2007).
13. H. T. Valentine, A. R. Ludlow, G. M. Furnival, Modeling crown rise in even-aged stands of Sitka spruce or loblolly pine. *For. Ecol. Manag.* **69**, 189–197 (1994).
14. A. Mäkelä, A carbon balance model of growth and self-pruning in trees based on structural relationships. *For. Sci.* **43**, 7–24 (1997).
15. D. A. Maguire, D. W. Hann, Constructing models for direct prediction of 5-year crown recession in southwestern Oregon Douglas-fir. *Can. J. For. Res.* **20**, 1044–1052 (1990).
16. D. G. Sprugel, T. M. Hinckley, W. Schaap, The theory and practice of branch autonomy. *Annu. Rev. Ecol. Syst.* **22**, 309–334 (1991).
17. T. J. Albaugh, H. L. Allen, T. R. Fox, Individual tree crown and stand development in *Pinus taeda* under different fertilization and irrigation regimes. *For. Ecol. Manag.* **234**, 10–23 (2006).
18. F. Minunno *et al.*, Bayesian calibration of a carbon balance model PREBAS using data from permanent growth experiments and national forest inventory. *For. Ecol. Manag.* **440**, 208–257 (2019).
19. D. Medvigy, S. C. Wofsy, J. W. Munger, D. Y. Hollinger, P. R. Moorcroft, Mechanistic scaling of ecosystem function and dynamics in space and time: Ecosystem Demography model version 2. *J. Geophys. Res. Biogeosci.* **114**, G1 (2009).
20. L. H. Reineke, Perfecting a stand-density index for even-aged forests. *J. Agric. Res.* **46**, 627–638 (1933).
21. P. Koivisto, Growth and yield tables. *Commun. Inst. For. Fenn.* **51**, 1–49 (1959) (In Finnish with English summary).
22. C. E. Prescott *et al.*, Surplus carbon drives allocation and plant–soil interactions. *Trends. Ecol. Evol.* **35**, 1110–1118 (2020).
23. J. F. Needham *et al.*, Tree crown damage and its effects on forest carbon cycling in a tropical forest. *Glob. Change. Biol.* **28**, 5560–5574 (2022).
24. M. E. Harmon *et al.*, Ecology of coarse woody debris in temperate ecosystems. *Adv. Ecol. Res.* **15**, 133–302 (1986).
25. S. Adu-Bredu, A. Hagihara, Long-term carbon budget of the above-ground parts of a young hinoki cypress (*Chamaecyparis obtusa*) stand. *Ecol. Res.* **18**, 165–175 (2003).
26. D. Kim, D. Medvigy, C. A. Maier, K. Johnsen, S. Palmroth, Biomass increases attributed to both faster tree growth and altered allometric relationships under long-term carbon dioxide enrichment at a temperate forest. *Glob. Change. Biol.* **26**, 2519–2533 (2020).
27. S. G. Pritchard, A. E. Strand, M. L. McCormack, M. A. Davis, R. Oren, Mycorrhizal and rhizomorph dynamics in a loblolly pine forest during 5 years of free-air-$CO_2$-enrichment. *Glob. Chang. Biol.* **14**, 1252–1264 (2008).
28. P. C. Stoy *et al.*, An evaluation of models for partitioning eddy covariance-measured net ecosystem exchange into photosynthesis and respiration. *Agric. For. Meteorol.* **141**, 2–18 (2006).
29. P. Muukkonen, A. Lehtonen, Needle and branch biomass turnover rates of Norway spruce (*Picea abies*). *Can. J. For. Res.* **34**, 2517–2527 (2004).
30. C. M. Hoover, Ed., *Field Measurements for Forest Carbon Monitoring: A Landscape-scale Approach* (Springer Science + Business Media, 2008).
31. S. Palmroth *et al.*, Nitrogen supply and other controls of carbon uptake of understory vegetation in a boreal *Picea abies* forest. *Agric. For. Meteorol.* **276–277**, 107620 (2019).
32. H. Lim, B. A. Olsson, T. Lundmark, J. Dahl, A. Nordin, Effects of whole-tree harvesting at thinning and subsequent compensatory nutrient additions on carbon sequestration and soil acidification in a boreal forest. *GCB Bioenergy* **12**, 992–1001 (2020).

33. H. Lim *et al.*, Inter-annual variability of precipitation constrains the production response of boreal *Pinus sylvestris* to nitrogen fertilization. *For. Ecol. Manag.* **348**, 31–45 (2015).
34. H. Lim *et al.*, Annual climate variation modifies nitrogen induced carbon accumulation of *Pinus sylvestris* forests. *Ecol. Appl.* **27**, 1838–1851 (2017).
35. R. Lutter *et al.*, Belowground resource utilization in monocultures and mixtures of Scots pine and Norway spruce. *For. Ecol. Manag.* **500**, 119647 (2021).
36. E. Holmström *et al.*, Productivity of Scots pine and Norway spruce in central Sweden and competitive release in mixtures of the two species. *For. Ecol. Manag.* **429**, 287–293 (2018).
37. R. Blaško, B. Forsmark, M. J. Gundale, T. Lundmark, A. Nordin, Impacts of tree species identity and species mixing on ecosystem carbon and nitrogen stocks in a boreal forest. *For. Ecol. Manag.* **458**, 117783 (2020).
38. M. C. Tyree, J. R. Seiler, C. A. Maier, K. H. Johnsen, *Pinus taeda* clones and soil nutrient availability: Effects of soil organic matter incorporation and fertilization on biomass partitioning and leaf physiology. *Tree. Physiol.* **29**, 1117–1131 (2009).
39. O. C. Campoe *et al.*, Climate and genotype influences on carbon fluxes and partitioning in Eucalyptus plantations. *For. Ecol. Manag.* **475**, 118445 (2020).
40. K. M. Littke *et al.*, Douglas-fir biomass allocation and net nutrient pools 15–20 years after organic matter removal and vegetation control. *Forests* **11**, 1022 (2020).
41. T. B. Harrington, R. A. Slesak, J. P. Dollins, S. H. Schoenholtz, D. H. Peter, Logging-debris and vegetation-control treatments influence competitive relationships to limit 15-year productivity of coast Douglas-fir in western Washington and Oregon. *For. Ecol. Manag.* **473**, 118288 (2020).
42. R. Lutter, A. Tullus, A. Kanal, T. Tullus, H. Tullus, The impact of short-rotation hybrid aspen (*Populus tremula L.* × *P. tremuloides Michx.*) plantations on nutritional status of former arable soils. *For. Ecol. Manag.* **362**, 184–193 (2016).
43. A. Tullus, K. Rosenvald, R. Lutter, A. Kaasik, P. Kupper, Coppicing improves the growth response of short-rotation hybrid aspen to elevated atmospheric humidity. *For. Ecol. Manag.* **459**, 117825 (2020).
44. R. Deshar *et al.*, Self-thinning exponents for partial organs in overcrowded mangrove *Bruguiera gymnorrhiza* stands on Okinawa Island, Japan. *For. Ecol. Manag.* **278**, 146–154 (2012).
45. J. Bergh, U. Nilsson, H. Grip, P.-O. Hedwall, T. Lundmark, Effects of frequency of fertilisation on production, foliar chemistry and nutrient leaching in young Norway spruce stands in Sweden. *Silva Fennica* **42**, 721–733 (2008).
46. R. Blaško *et al.*, The carbon sequestration response of aboveground biomass and soils to nutrient enrichment in boreal forests depends on baseline site productivity. *Sci. Total. Environ.* **838**, 156327 (2022).
47. J. Bergh, S. Linder, T. Lundmark, B. Elfving, The effect of water and nutrient availability on the productivity of Norway spruce in northern and southern Sweden. *For. Ecol. Manag.* **119**, 51–62 (1999).
48. H. Lim *et al.*, Boreal forest biomass accumulation is not increased by two decades of soil warming. *Nat. Clim. Change.* **9**, 49–52 (2019).
49. M. Näslund, Empirical formulae and tables for determining the volume of standing trees: Scots Pine, Norway Spruce and Birch in southern Sweden and in the whole of the country. *Meddelanden Fran Statens Skogsforskningsinstitut* **36**, 81 (1947), (in Swedish).
50. F. Minunno *et al.*, Bayesian calibration of a carbon balance model PREBAS using data from permanent growth experiments and national forest inventory. *For. Ecol. Manag.* **440**, 208–257 (2019).
51. H. McCarthy *et al.*, Re-assessment of plant carbon dynamics at the Duke free-air $CO_2$ enrichment site: Interactions of atmospheric [$CO_2$] with nitrogen and water availability over stand development. *New. Phytol.* **185**, 514–528 (2010).
52. H. T. Valentine, A. Mäkelä, Bridging process-based and empirical approaches to modeling tree growth. *Tree. Physiol.* **25**, 769–779 (2005).
53. M. Peltoniemi *et al.*, A semi-empirical model of boreal forest gross primary production, evapotranspiration, and soil water-calibration and sensitivity analysis. *Boreal. Env. Res.* **20**, 151–171 (2015).
54. M. Hu, F. Minunno, M. Peltoniemi, A. Akujärvi, A. Mäkelä, Testing the application of process-based forest growth model PREBAS to uneven-aged forests in Finland. *For. Ecol. Manag.* **529**, 120702 (2023).
55. F. Minunno *et al.*, Calibration and validation of a semi-empirical flux ecosystem model for coniferous forests in the Boreal region. *Ecol. Model.* **341**, 37–52 (2016).
56. A. Mäkelä, H. T. Valentine, *Models of Tree and Stand Dynamics. Theory, Formulation and Application* (Springer Nature, 2020), p. 310.
57. A. K. Cajander, Finnish forest types and their significance. *Acta. For. Fenn.* **56**, 1–71 (1949).
58. M. Longo *et al.*, The biophysics, ecology, and biogeochemistry of functionally diverse, vertically and horizontally heterogeneous ecosystems: The Ecosystem Demography model, version 2.2–Part 1: Model description. *Geosci. Model. Dev.* 12, 4309–4346 (2019).
59. D. Medvigy, S. C. Wofsy, J. W. Munger, P. R. Moorcroft, Responses of terrestrial ecosystems and carbon budgets to current and future environmental variability. *Proc. Natl. Acad. Sci. U.S.A* **107**, 8275–8280 (2010).
60. A. T. Trugman *et al.*, Climate, soil organic layer, and nitrogen jointly drive forest development after fire in the North American boreal zone. *J. Adv. Model. Earth. Syst.* **8**, 1180–1209 (2016).
61. X. Xu, D. Medvigy, J. S. Powers, J. M. Becknell, K. Guan, Diversity in plant hydraulic traits explains seasonal and inter-annual variations of vegetation dynamics in seasonally dry tropical forests. *New. Phytol.* **212**, 80–95 (2016).
62. D. Medvigy *et al.*, Observed variation in soil properties can drive large variation in modelled forest functioning and composition during tropical forest secondary succession. *New. Phytol.* **223**, 1820–1833 (2019).
63. M. Longo *et al.*, The biophysics, ecology, and biogeochemistry of functionally diverse, vertically and horizontally heterogeneous ecosystems: The Ecosystem Demography model, version 2.2–Part 2: Model evaluation for tropical South America. *Geosci. Model. Dev.* **12**, 4347–4374 (2019).
64. N. B. Schwartz *et al.*, Intra-annual variation in microclimatic conditions in relation to vegetation type and structure in two tropical dry forests undergoing secondary succession. *For. Ecol. Manag.* **511**, 120132 (2022).
65. A. A. Gonzalez-Benecke *et al.*, Local and general above-stump biomass functions for loblolly pine and slash pine trees. *For. Ecol. Manag.* **334**, 254–276 (2014).
66. J. Repola, Biomass equations for Scots pine and Norway spruce in Finland. *Silva Fenn.* **43**, 625–647 (2009).
67. J. Muñoz Sabater, Data from "ERA5-Land monthly averaged data from 1981 to present, Copernicus Climate Change Service (C3S) Climate Data Store (CDS)". Available at: https://cds.climate.copernicus.eu/cdsapp#!/search?type=dataset&text=era5-land.
68. H. Lim, Field-based datasets for estimation of forest branch biomass turnover. safedeposit. https://www.safedeposit.se/projects/484. Deposited 27 September 2024.